Research Article

Ali İhsan Çelik, Ufuk Tunç, Memduh Karalar, Essam Althaqafi, and Yasin Onuralp Özkılıç*

Sustainable utilization of aluminum waste in geopolymer concrete: Influence of alkaline activation on microstructure and mechanical properties

https://doi.org/10.1515/rams-2025-0152
received April 03, 2025; accepted August 21, 2025

Abstract: The study investigated the impact of incorporating varying quantities of aluminum waste (Al-waste) and slag on the properties of geopolymer concrete, specifically by altering the molarity (M) and Al-waste. To achieve this objective, slag was substituted with fly ash at 0, 5, 10, and 20% concentrations. Furthermore, oven and ambient curing were compared. The impact of M was subsequently examined. The study also includes the examination of penetrability, time of setting, compressive strength tests, splitting tensile tests, and flexural strength tests. An increase in M was found to result in a decrease in the penetrability of the mixture. The findings indicated a negative correlation between the slump values and both the M and Al-waste ratios, and a rise in both factors led to a drop in slump values. Although Al-waste had improved at the time of setting, M still had a substantial impact. Although high M enhanced the mechanical strength, it had a significant negative influence on the setting time and penetrability. This investigation demonstrated that Al-waste had a slight negative influence on the mechanical strength and penetrability. In addition, scanning electron microscopy, thermal gravimetric analysis, and energy dispersive X-ray examination were carried out.

Keywords: geopolymer concrete, recycling, aluminum waste, expanded and lightweight concrete penetrability, time of setting, compressive, flexural, splitting, ambient

Abbreviation

Al-waste	aluminum waste
CS	compressive strength
DTA	differential thermal analysis
DTG	derivative thermogravimetry
EDX	energy dispersive X-ray
FA	fly ash
FS	flexural strength
GP	geopolymer
GPC	geopolymer concrete
M	molarity
OPC	ordinary Portland concrete
SEM	scanning electron microscopy
SF	silica fume
STS	splitting tensile strength
TGA	thermal gravimetric analysis

*** Corresponding author: Yasin Onuralp Özkılıç,** Department of Civil Engineering, Necmettin Erbakan University, Konya, Turkey; Department of Unique Buildings and Constructions Engineering, Don State Technical University, Gagarin Sq. 1, Rostov-on-Don, 344003, Russia; Department of Technical Sciences, Western Caspian University, 1001, Baku, Azerbaijan, e-mail: yozkilic@erbakan.edu.tr
Ali İhsan Çelik, Ufuk Tunç: Department of Construction, Kayseri Üniversitesi Tomarza Mustafa Akincioglu Vocational School, Kayseri University, Kayseri, 38940, Turkey
Memduh Karalar: Department of Civil Engineering, Zonguldak Bulent Ecevit University, Zonguldak, Turkey
Essam Althaqafi: Civil Engineering Department, College of Engineering, King Khalid University, Abha 61421, Saudi Arabia

1 Introduction

The production of Portland cement used in concrete and its raw materials has numerous ecological influences, including CO_2 release, natural source exhaustion as well as fossil fuel consumption. To eliminate these environmental problems, sustainable cementitious supplies are being developed with the purpose of decreasing or replacing the Portland cement content. Sustainable cementitious materials are being developed to reduce or completely

Open Access. © 2025 the author(s), published by De Gruyter. This work is licensed under the Creative Commons Attribution 4.0 International License.

replace the Portland cement component. Recently created clinker methods, using carbonation instead of hydration for concrete production, may diminish net CO_2 emissions by up to 70% relative to Portland cement clinker and are already commercially accessible in some regions [1,2]. According to the research, one of the methods that can be used to reduce the impact of this factor is to increase the consumption of auxiliary materials like fly ash (FA), slag, and silica fume (SF), all of which significantly lower the required amount of Portland cement. The use of other cementitious materials as a partial or total replacement for Portland cement in the concrete mix is a second approach. Geopolymer (GP) is recognized as one of the most promising options [3]. GPs might be prepared from several kinds of aluminosilicate resources, including coal ash, SF, calcined clay, and/or alumina [4]. Furthermore, for the manufacturing of geopolymer concrete (GPC), FA, granulated blast furnace slag (GBFS), and metakaolin each of which have a high silica and alumina content are the often used ingredients [5]. The calcined clays (metakaolin) and industry Al-wastes (FA and GBFS) are the two types of aluminosilicate materials that are used most often in the production of GP binders [6]. More research must be done on the method of geopolymerization that involves the consumption of waste materials, so that the sources of clay that occur naturally may be preserved and the process can realize its full profit potential. The utilization of waste materials, particularly the industrial Al-waste in GP, has demonstrated positive effects on mechanical strength, workability, and environmental sustainability; moreover, the influence of different curing conditions on these performances is highlighted in the literature [7–12].

Gülmez [13] examined the investigative consequences of the influence of industrial Al-wastes on the behavior of cementitious mixtures. For that reason, the influence of Al-waste on the physical and mechanical properties of cement-based mixtures was evaluated. The results showed that the mixtures containing 4% Al aggregates had the maximum water absorption and porosity. It has been shown that combining Al-waste into mixtures might be a proper solution for recycling in industrial applications. Ozkilic *et al.* [14] utilized Al lathe waste to produce expansive concrete by substituting aggregates in specific proportions with recycled materials. As part of the investigation work, five distinct types of Al-wastes were chosen at concentrations of 1, 2, 3, 4, and 5% for the purpose of comparison. An additional Al-waste that did not include any Al was created as a reference type. When the Al volume percentage was more than 2%, it was noticed that the material's workability dramatically diminished. This was a consequence of the mechanical tests that were conducted. Another research was carried out by Almeshal *et al.* [15] to examine the performance of reinforced concrete beams that were mixed with Al-waste. The casting and testing of a total of 12 reinforced concrete beams were carried out with varying degrees of low reinforcement ratios (0.0125, 0.0074, and 0.0032) and Al-waste ratios (1, 2, and 3%). When 1 and 2% Al-wastes were added to concrete, it was found that the load-bearing ability of the concrete did not change. However, when 3% Al-waste was added, the load capacity of concrete beams reduced by 8–20%. An investigation was conducted by Özkılıç *et al.* [16] to examine the impact of varying quantities of AL-waste material on the shear behavior of the beam used in the study. It was determined that the maximum load, stiffness, ductility, and energy dissipation capability of each sample were determined *via* the use of experiments for Al-waste ratios (1, 2, and 3%). It is worth noting that the optimum capacity of the beams decreases as the proportion of Al-waste in the concrete mixture increases. Mohammadyan-Yasouj *et al.* [17] examined the impact of nano-alumina powder on self-compacting concrete at elevated temperatures. To achieve this objective, three mixture designs were examined at temperatures of 27, 100, 200, 300, 450, and 600°C: without the cement substitute nano-alumina, with 1% nano-alumina, and with 2% nano-alumina. Based on the experimental findings, it was observed that the pozzolanic activity of nano-alumina enhanced the compressive strength (CS) of specimens of concrete both at room temperature and below 100°C. After being subjected to a heating process for 10 min, the CS of 28 day samples that included 1% nano-alumina and 2% nano-alumina was found to be 11.7 and 16.2% greater than the reference sample, respectively. The other investigation was performed by Rahim *et al.* [18]. In this investigation, it was studied what would happen if recyclable Al components were used in place of sand in the concrete mixture at 1, 2, and 5%, respectively. Upon completion of the investigation, it was determined that the samples containing 1% Al-waste exhibited superior strength, whereas the samples containing 5% Al-waste exhibited robust resistance to water absorption.

The literature has a variety of research about the use of GPC. Bumanis *et al.* [19] examined the performance of two distinct porous GPs derived from waste clay and salt slag ingredients. The acquired GP was detailed in terms of its physical and mechanical properties. The CS outcomes for GPs that are based on illite clay might hint at the effect of salt slag on the strength of the GP matrix when increased quantity of Al-waste was introduced into the arrangement. Furthermore, it was obtained that illite clay-based GP

presented better performance with improved salt cake content, which points out that salt cake contributes to alkali activation with its Al-waste influence, causing a more stable GP arrangement. Onutai *et al.* [20] performed an investigation to examine the mixture of the dense and porous configurations of GP using FA and industry Al-waste as raw materials. For this purpose, Al-waste and FA were selected to mix into dense GPs for cement materials. At the end of this investigation, it was found that the Al-waste-based GP affected the GP strength, and that variations in sodium hydroxide (NaOH) concentration induced by changes in curing temperatures also played a role. Furthermore, it was observed that additional Al-waste produced a reduction in GP strength. The other investigation was performed by Onutai *et al.* [21]. In this study, Onutai *et al.* [21] defined the reprocessing of Al-waste for GPs. For this purpose, both Al-waste and FA were combined in dissimilar Al-waste contents of 10–60 wt%. Then, the mechanical properties, microstructure, bonding, and stages of the resultant GPs were determined. It was found that the Al-waste ingredient in the GP affected the GP strength and NaOH concentration was altered at dissimilar curing temperatures. It was found that FA and Al-waste were suitable sources for GP materials. To define the influence of mineral content on the CS of the generated GP, Xu and Van Deventer [22] monitored the geopolymerization of 15 naturally occurring Al–Si minerals. This research demonstrates that a wide variety of naturally occurring Al–Si minerals have the potential to serve as sources for producing GPs. Kouamo *et al.* [23] associated the properties of GPs prepared from metakaolin and volcanic ash and examined the influence of adding Al_2O_3 to metakaolin and volcanic ash-based GPs at ambient temperature. The consequences demonstrate that both metakaolin and volcanic ash might be used as base materials for the manufacture of GPs. Furthermore, the properties of volcanic ash-based GP, might be enhanced, while alumina was consumed to supply the insufficient Al_2O_3 content in the volcanic ash. Oderji *et al.* [24] performed an investigational study to define the mechanical properties of the GPs. For this purpose, different alkali activators were used, and an analysis was conducted to present the optimum amount and type of activator for a one-part FA-based GP. The CS of one-part GP binders significantly decreased with the reduction of sodium silicate content.

As noted in previous examinations, there are some research in the literature [24–30] on the role of GP in consuming alumina resources. On the other hand, in the literature, insufficient investigations were recognized on the effects of different percentages of Al-waste. Additionally, there are very limited investigations on the impact of Al-waste in GPC. Consequently, the study makes several significant contributions to the existing body of research. In the parts that follow, information will be presented.

1.1 Importance of study

Literature evaluation has shown a need for more research on the use of GPC, particularly with the incorporation of Al-waste. Moreover, a literature review indicates that the limited investigation on GPC has mostly focused on curing techniques. Research on the use of both ambient and oven-curing techniques in GPC is lacking. Additional research is required owing to the distinct advantages and challenges linked to GPC. This study is significant because it investigates the impact of different compounds on GPs, given that the curing process is a crucial factor. Thus, in this study, the effect of different curing methods (ambient and oven) on the strength of GPC was investigated, and mechanical properties were evaluated. Another aim of this study is to expand the knowledge of this material by investigating the machinability and strength of GPC produced by partially replacing slag with FA. The experiment detailed here aims to address these disparities by examining the impacts of Al-waste and the percentage of slag on various mechanical properties, durability, and fresh properties of FA-based GPC specimens. Since ambient curing of GPC is considered a feasible alternative for ordinary Portland concrete (OPC), efforts in this field are encouraged. This research was conducted to assess the influence of the granulated blast furnace slag ratios 0, 5, 10, and 20%.

2 Experimental program

In this study, GPC was manufactured using Al-waste. A total of 43 different mix ratio samples were produced. For each mix ratio, three specimens were prepared and tested. The results presented represent the average values of these three replicates. Sixteen samples do not contain Al-waste and are characterized as reference samples. The remaining 27 samples were obtained by adding different amounts of Al-waste. Al-waste was obtained from a CNC machine utilized in the laboratory. The sizes of Al-waste particles were found to range approximately between 15 and 30 mm. For this purpose, five different ratios of Al-waste (0, 1, 2, 3 and 4%) were used. In addition, slag was used to assess the curing performance of the GPC both in the environment and in the furnace. Some of the samples to which slag was added were cured outdoors and some in the oven. Binding materials, aggregates, and alkali activators used in the study are shown in Figure 1.

Figure 1: Experimental materials.

The flowchart of this work is shown in detail in Figure 2. Alkaline activators, binders, and aggregates are the three main categories of materials for obtaining GPC. The materials used in each category are shown in their respective sub-components. NaOH and sodium silicate as alkali activators are indispensable for GPC. Although FA is the main binder material, a certain amount of ground blast furnace slag is added to cure outdoors. The most original contribution of the study is Al-waste. The addition of Al in the production of structural GPC is a new area of study.

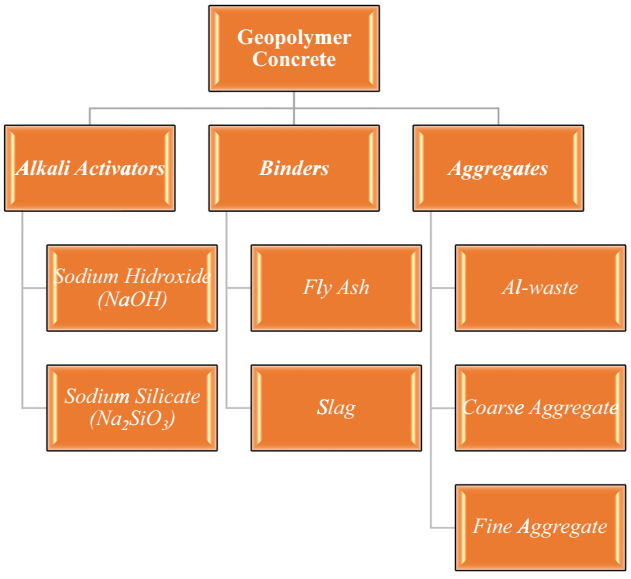

Figure 2: Flow chart of GPC production.

Details showing the mixing ratios and curing conditions of the study are given in Table 1. In GPC concrete production, the M is an essential requirement to obtain the desired mechanical performance of the concrete. It is known that as the M increases, concrete strength increases, and as M decreases, concrete strength decreases [26,27]. However, the increase in M reduces the penetrability of fresh concrete. There are studies in the literature up to 8–18 M [28,29,31,32]. Considering the penetrability and strength of the GPC samples obtained, 11, 13, and 16 M were used in this study. Higher M study is not possible because the high calcium content in slag consumes the solutions very quickly.

Table 2 presents the chemical compositions of FA and blast furnace slag waste materials used as binding materials. The most important reason for using blast furnace slag in the study is that it provides GPC resistance in a short time under ambient curing conditions, thanks to the high CaO it contains. The slag ratio was determined by research done at Erciyes University, Taum Laboratory.

To ensure a consistent blend, researchers utilized a laboratory concrete mixer. The compression and shaking operations were carried out, while the GPC was being poured into the concrete molds. Following the molding process, the GP mixes were allowed to cure among the environment. The ambient cured samples were exposed to open air in the Sun, while oven cured samples were exposed to a 24 h curing method in an oven at 85°C. Previous studies have demonstrated that mixtures containing slag are capable of achieving sufficient strength development under ambient conditions [33]. In contrast, systems without slag generally require

Table 1: GPC mix materials

Sample no.	FA (g)	Slag (g)	Al-waste (g)	Na_2SiO_3 (g)	NaOH (g)	Fine aggregate (g)	Coarse aggregate (g)	Al-waste Ratio (%)	NaOH Molarity (M)	Curing method
1	1527.4	80.37	0	573.96	229.57	2545.25	4726.34	0	13	Ambient
2	1446.93	160.77	0	573.96	229.57	2545.25	4726.34	0	13	Ambient
3	1286.16	321.54	0	573.96	229.57	2545.25	4726.34	0	13	Ambient
4	1527.4	80.37	75	573.96	229.57	2545.25	4726.34	1	13	Ambient
5	1446.93	160.77	75	573.96	229.57	2545.25	4726.34	1	13	Ambient
6	1286.16	321.54	75	573.96	229.57	2545.25	4726.34	1	13	Ambient
7	1527.4	80.37	75	573.96	229.57	2545.25	4726.34	1	11	Ambient
8	1446.93	160.77	75	573.96	229.57	2545.25	4726.34	1	11	Ambient
9	1286.16	321.54	75	573.96	229.57	2545.25	4726.34	1	11	Ambient
10	1527.4	80.37	75	573.96	229.57	2545.25	4726.34	1	16	Ambient
11	1446.93	160.77	75	573.96	229.57	2545.25	4726.34	1	16	Ambient
12	1286.16	321.54	75	573.96	229.57	2545.25	4726.34	1	16	Ambient
13	1527.4	80.37	150	573.96	229.57	2545.25	4726.34	2	13	Ambient
14	1446.93	160.77	150	573.96	229.57	2545.25	4726.34	2	13	Ambient
15	1286.16	321.54	150	573.96	229.57	2545.25	4726.34	2	13	Ambient
16	1527.4	80.37	225	573.96	229.57	2545.25	4726.34	3	13	Ambient
17	1446.93	160.77	225	573.96	229.57	2545.25	4726.34	3	13	Ambient
18	1286.16	321.54	225	573.96	229.57	2545.25	4726.34	3	13	Ambient
19	1527.4	80.37	300	573.96	229.57	2545.25	4726.34	4	13	Ambient
20	1446.93	160.77	300	573.96	229.57	2545.25	4726.34	4	13	Ambient
21	1286.16	321.54	300	573.96	229.57	2545.25	4726.34	4	13	Ambient
22	1607.77	0	0	573.96	229.57	2545.25	4726.34	0	11	Ambient
23	1527.4	80.37	0	573.96	229.57	2545.25	4726.34	0	11	Ambient
24	1446.93	160.77	0	573.96	229.57	2545.25	4726.34	0	11	Ambient
25	1286.16	321.54	0	573.96	229.57	2545.25	4726.34	0	11	Ambient
26	1607.77	0	0	573.96	229.57	2545.25	4726.34	0	13	Ambient
27	1607.77	0	0	573.96	229.57	2545.25	4726.34	0	16	Ambient
28	1527.4	80.37	0	573.96	229.57	2545.25	4726.34	0	16	Ambient
29	1446.93	160.77	0	573.96	229.57	2545.25	4726.34	0	16	Ambient
30	1286.16	321.54	0	573.96	229.57	2545.25	4726.34	0	16	Ambient
31	1607.77	0	0	573.96	229.57	2545.25	4726.34	0	13	Oven
32	1527.4	80.37	0	573.96	229.57	2545.25	4726.34	0	13	Oven
33	1446.93	160.77	0	573.96	229.57	2545.25	4726.34	0	13	Oven
34	1286.16	321.54	0	573.96	229.57	2545.25	4726.34	0	13	Oven
35	1527.4	80.37	75	573.96	229.57	2545.25	4726.34	1	13	Oven
36	1446.93	160.77	75	573.96	229.57	2545.25	4726.34	1	13	Oven
37	1286.16	321.54	75	573.96	229.57	2545.25	4726.34	1	13	Oven
38	1527.4	80.37	75	573.96	229.57	2545.25	4726.34	1	11	Oven
39	1446.93	160.77	75	573.96	229.57	2545.25	4726.34	1	11	Oven
40	1286.16	321.54	75	573.96	229.57	2545.25	4726.34	1	11	Oven
41	1527.4	80.37	75	573.96	229.57	2545.25	4726.34	1	16	Oven
42	1446.93	160.77	75	573.96	229.57	2545.25	4726.34	1	16	Oven
43	1286.16	321.54	75	573.96	229.57	2545.25	4726.34	1	16	Oven

curing at elevated temperatures, typically between 60 and 90°C, to attain early strength [34]. Accordingly, the curing temperatures and durations used in this study were determined based on preliminary tests and consistency with findings reported in the literature.

Since GPC was formed by activating chemical components such as alumina and silicate, it is possible to achieve the necessary strength and durability by curing it in an oven. GPC oven curing needs to be done quickly and in a controlled manner. The application process and conditions may vary depending on the concrete mix used, the intended application, and the specific requirements. In the literature, there are oven-curing studies from 40 to 110°C [35–37]. As the temperature increases, the GPC strength also increases; however, high temperatures are known to cause excessive embrittlement at temperatures above 90°C. From this point of view, 40 mm ×

Table 2: Component values of FA blast furnace slag materials [28]

Component	FA%	Slag%
SiO_2	57.3	18.20
Al_2O_3	24.9	7.5
Fe_2O_3	6.05	0.1
CaO	3.98	67.60
SO_3	0.47	0.76
Na_2O	1.24	—
Cl^-	0.05	—
MnO	—	0.44
K_2O	—	0.76
TiO_2	—	0.95
NiO_3	—	0.04
SrO	—	0.019
ZrO_2	—	0.082
Sledge (>45 μm)	17.4	0

40 mm × 160 mm prism and 100 mm × 200 mm cylindrical specimens were prepared, and these specimens were cured at 85° for 24 h (Figure 3). After curing in the oven, the samples were removed and kept outside for 28 days to be tested.

3 Discussion on experimental outcomes

3.1 Penetrability and setting time

The penetrability of the mixture was reduced with the increase in the M of NaOH. This behavior was observed in numerous studies in the literature. Nevertheless, in this investigation, it was found that the addition of Al-waste led to a reduction in the slump values and improved the penetrability of the material. It was noted that the time of setting was around 10 min with 1, 2, and 3% Al-waste addition and 40 min with 4% addition. The consequences were consistent with similar investigations in the literature. Based on Yip and Van Deventer [38], there is evidence that the presence of calcium throughout the mixture of FA-based GPC enhances the likelihood of forming compounds such as calcium silicate and calcium aluminate hydrates. This information comes from studies that have been conducted [36]. Alkali-activated concrete might be compressed well on a vibrating table even for comparatively low slump values. Consequently, the penetrability of alkali-activated concrete is categorized and established on the form of compaction [39].

3.2 Slump test

Based on studies collected from prior examinations and experience obtained during the procedure, it was observed that permeability dramatically reduces as both the M of NaOH increased. The results indicated that the slump values declined as M increased. Conversely, maintaining a constant M allowed for the investigation of how the amount of Al-wastes affected the slump. While the NaOH content was selected as 11 M, it was revealed that the slump values decreased as the Al-waste content proportion increased from 0 to 1%, indicating a correlation between

Figure 3: Curing of GPC samples and weight control.

the two parameters. The same observation was made for 13 M when considering it as the AL percentage. It was revealed that the value of the slump grew when the percentage of Al-waste contents improved from 0 to 1%. When the Al content increased from 1 to 4%, a reduction in slump values was observed. The same observation was made for 16 M when the Al proportion was altered. It was found that the slump values increased as the Al-waste content proportion improved from 0 to 1%.

While the amount of Al-waste increased by 0–4%, there was a significant decrease in slump values. Specifically, the slump decreased to 40–60 mm with 1% Al, 15–40 mm with 2% Al, and 5–10 mm with 3–4% Al. Al reacts with water in an alkaline environment, especially in systems containing NaOH, to produce hydrogen gas (H_2). This reaction causes gas bubbles to form in the concrete, causing the mix to expand in volume. At the same time, this outgassing destabilizes the consistency of the mixture, reducing cohesion and workability. The irregular, sharp, wiry geometry of the chip particles and their low specific gravity reduce the cohesion of the concrete and require more water. However, since no additional water is added, the slump decreases. As the slag ratio increases in the mixture, an increase in slump values is observed, especially in Al-free or low Al ratio samples. However, this positive effect disappears in specimens containing slag and high Al-waste. Slag is a reactive binder that dissolves particularly well in alkaline media, forming binder gels such as calcium-aluminosilicate-hydrate (C–A–S–H) and sodium-aluminosilicate-hydrate (N–A–S–H). This generally enhances the workability. However, in the presence of Al-waste, the positive effect of slag is suppressed because the resulting hydrogen gas and rapid reactions destabilize the mixture.

Examining the chemical composition of the slag in Table 2 reveals a particularly high amount of calcium oxide (CaO). This indicates that, in addition to the dominant N–A–S–H gel phase found in the traditional low-calcium GP systems, other phases, such as C–A–S–H, may also form. These hybrid structures have a twofold effect on long-term stability. First, a rapid increase in mechanical strength occurs at early ages due to the presence of C–A–S–H phases. This significantly improves the performance of the binder, especially in systems cured at ambient temperature. Conversely, the possibility of carbonation and other chemical deterioration in alkaline environments increases with higher calcium content, which may limit long-term durability. The study emphasizes that the slag additive facilitates ambient-temperature curing. However, it does not present measurements such as the strength activity index (SAI) or thermal reactivity profiles based on isothermal calorimetry, which would quantitatively reveal the effectiveness of slag in the binder system. Therefore, additional characterizations are needed to clarify whether the slag additive creates a synergistic binder structure with the GP matrix. Future studies can perform tests such as separating heat flows in hydration and geopolymerization processes by isothermal calorimetry.

3.3 A thorough examination of the compressive test

As can be seen from Table 3, the properties are highly dependent on the relative amounts of NaOH and Al-waste ratio, in addition to the temperature at which they are cured [40–43]. In the context of this inquiry, it is important to observe the required curing temperature and NaOH concentration. The CS was in GPC that was prepared by combining various amounts of aluminum hydroxide and NaOH. These GPCs were structured such that the concentrations of both variables varied. It was discovered that there was a pattern in which the strength of the GPC enhanced as the concentration of NaOH increased. As shown in Figure 4, the concentrations of 11, 13, and 16 M NaOH produced the highest strength in the CS when the CS contained 0% of Al-waste. The M of NaOH was fixed at 11, while the proportion of slag ratio was adjusted to 0, 5, 10, and 20% in the GPC mixture. In addition, the ratio of this factor was changed from 0 to 1% in the calculation of the mixture modified with the ratio of Al-waste aggregate, which included FA. This was done to reflect that the ratio was changed. At the end of this procedure, the ratio of variation in CS was determined to be 17.66% (from 20.28 to 16.697 MPa for 5% slag ratio). While the percentage in

Table 3: CS test results for different NaOH and Al-waste % (MPa)

Al-waste (%)	Slag ratio 0%	Slag ratio 5%	Slag ratio 10%	Slag ratio 20%
NaOH (11 M)				
0	25.62	20.28	18.86	17.59
1	—	16.70	15.86	15.89
NaOH (13 M)				
0	26.59	22.33	21.02	19.23
1	—	18.10	17.60	16.45
2	—	16.62	15.77	14.14
3	—	14.28	13.65	12.41
4	—	12.88	11.19	10.32
NaOH (16 M)				
0	30.26	28.82	24.56	20.90
1	—	19.08	18.23	17.34

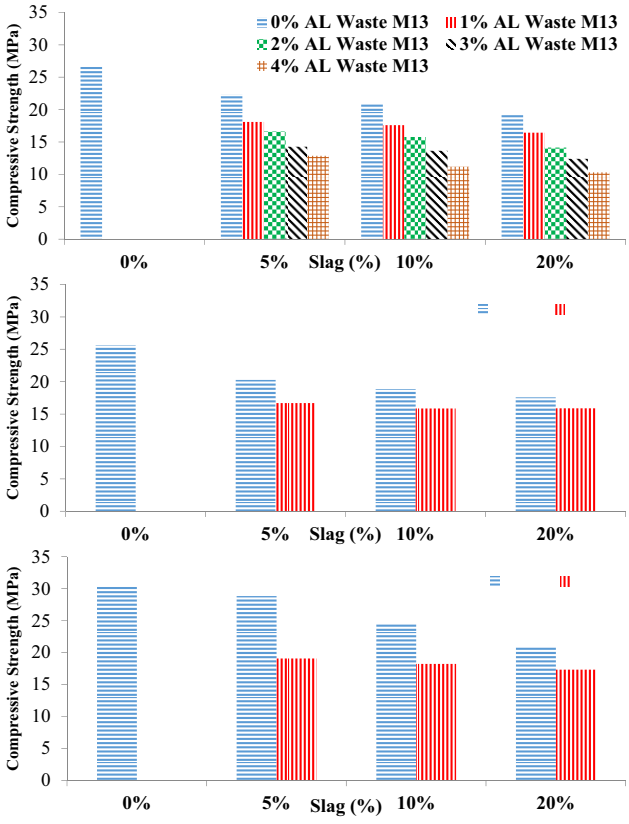

Figure 4: Results of the CS test.

the mixture was enhanced, it was observed that this quantity of variation reduced to approximately 15.90% (from 18.86 to 15.86 MPa for 10% slag ratio). While the percentage in the mixture was enhanced, it was observed that this quantity of variation reduces to approximately 9.66% (from 17.59 to 15.89 MPa for 20% slag ratio). Additionally, the M of NaOH was selected repeatedly at 13 M, and the percentage of slag ratio was changed to 0, 5, 10, and 20% in the GPC mixture. At this mixture, the percentage of variation in CS at 5% slag ratio was reduced as 18.9% (from 22.33 to 18.10 MPa). While the amount of Al-waste in this mixture increased to 4%, the amount of CS in the mixture decreased by around 42.32% (from 22.33 to 12.88 MPa). Similarly, while the slag ratio in the mixture was increased from 0 to 20%, it was discovered that there was a 27.7% reduction in the CS of the mixture (from 26.59 to 19.228 MPa). The mixture's CS had dropped by 46.3%, while the levels of Al-waste in the mixture increased from 0 to 4%, constituting 20% of the mixture's total volume.

In addition to this, the NaOH concentration was determined to be 16 M, supporting consistent findings. While the slag ratio in the mixture was improved from 0 to 20%, the CS of the mixture was observed to decrease by 30.93% (from 30.264 to 20.9 MPa). While the amount of Al-waste in the combination increased from 0 to 1%, resulting in a significant relative increase, the mixture's CS was determined to have decreased by 33.79% (from 28.82 to 19.08 MPa).

The outcomes of the CS test are provided in Table 3 as well. During these investigations, the percentage of Al-waste aggregate that was mixed with FA was calculated, and the molar concentration of NaOH in the mixture was varied to 11, 13, and 16 M to observe the effects of these changes. The results of these investigations are summarized in Table 3. As observed in Table 3, the calculation of the amount of the Al-waste aggregate with FA was incrementally occupied at 0, 1, 2, 3, and 4%, while the percentage of M of NaOH was increased incrementally from 11 to 13 M and then to 16 M in the mixture of concrete. It was observed that this percentage of variance tends to increase to 10.10% (from 11 to 13 M) and 42.11% (from 11 to 16 M) for Al-waste containing 0 and 5% slag ratios. When the Al-waste ratio increased by 1%, it was observed that this percentage of variance tends to increase to 8.40% (from 11 to 13 M) and to 14.27% (from 11 to 16 M) for Al-waste containing 1 and 5% slag ratios.

This may be because larger concentrations of NaOH can melt silica and alumina together into a homogeneous slurry paste [20]. Furthermore, it was found in earlier studies that while the GP contained increased Al-waste content, the strength was somewhat lower than that of 0 wt% [20]. Adding Al-waste influenced the alumina component in the matrix. The findings of this study are consistent with previous research findings. In another study, it was also observed that additional NaOH was the reason for the CS reduction, attributable to the aluminosilicate gel precipitation [43]. It was found that higher concentrations of NaOH retained the Na ions in GPC. Furthermore, the concentration of Ca decreased concomitantly with increasing NaOH concentration. This statement showed the Na component's inclination to exchange with the Ca component in the GP matrix [21].

3.4 Examination of the splitting tensile strength (STS)

The consequences of STS persistently follow the parallel trend as the CS, as shown in Figure 5. As shown in Table 4, the M of NaOH was consistently chosen at 11 M, whereas the inclusion of slag ratio in the concrete mixture was varied to 0, 5, 10, and 20% for the Al-waste aggregate. In the experimental design, the composition of the mixture was modified by increasing the proportion of Al-waste ratio from 0 to 1%. In addition, a consistent M value of 11 for NaOH was used, while the amount

of Al-waste aggregate mixed with FA was varied at 0, 5, 10, and 20%. For 11 M and 0% Al-waste rate, the decrease in STS values (from 0 to 20% slag ratio) is as follows. In this configuration, the proportion of variability in STS was 1.20, 4.12, and 9.45%. Moreover, a constant M ratio of NaOH at 13 was used, while the fraction of Al-waste aggregate mixed with FA in the GPC mixture was enhanced to 0, 5, 10, and 20%. In this instance, the percentage of variance in STS at a significant level of 5% was determined to be 6.44% (from 9.31 to 8.71 MPa). It was found that the STS of the mixture dropped by 35.18% as the slag ratio in the mixture increased from 5 to 20%. It was detected that the STS of the mixture decreased by 61.19%, while the quantities of Al-waste in the mixture were enhanced from 0 to 4% for 5% slag ratio and 13 M. Additionally, the M of NaOH was designated as 16 M. While the proportion of slag in the mixture was enhanced from 0 to 20%, it was detected that the STS of the mixture decreased by 5.46% (from 10.43 to 9.86).

During these investigations, the proportion of the Al-waste aggregate that included FA was maintained at a constant level, while the amount of NaOH in the mixture was varied to 11, 13, and 16 M, as shown in Table 4. Furthermore, as observed from Table 4, the percentage of Al-waste aggregate with FA was altered repetitively as 0, 1, 2, 3, and 4%, and the amount of M of NaOH was kept as 11, 13, and 16 M the concrete mixture. STS decreased as the M of the mixture increased. In Figures 5 and 6, STS test results are given.

Table 4: STS test results (MPa)

Al-waste (%)	Slag ratio 0%	Slag ratio 5%	Slag ratio 10%	Slag ratio 20%
NaOH (11 M)				
0	9.94	9.82	9.53	9.00
1	—	5.75	5.15	4.77
NaOH (13 M)				
0	9.31	8.71	8.15	7.74
1	—	7.14	6.57	5.85
2	—	6.42	5.80	4.79
3	—	4.99	4.25	3.38
4	—	3.78	3.26	2.45
NaOH (16 M)				
0	10.43	10.34	10.12	9.86
1	—	8.03	7.50	7.16

3.5 A comprehensive analysis of flexural behavior

The strength of samples that have been subject to flexure may be used as the tensile capability of GPC, when they are combined. Besides this, the flexural strength (FS) is generally greater than the indirect STS [44]. As detected from Table 5, 11 M was used as the M percentage of NaOH, and the ratio of slag ratio in the concrete mix was adjusted from 0 to 5%, 10%, and 20%, respectively. The percentage was improved from 0 to 20% in the design of the mixture, which was altered by adjusting the slag ratio. This modification occurred in the design of the mixture. Additionally, the value of M of NaOH was set as 11. While the proportion in the mix was enhanced, it was observed that this amount of variation tends to decrease. In this setup, the proportion of variation in FS was recognized to be 2.33, 6.61, and 10.11%.

The percentage was improved from 0 to 1% in the design of the mixture, which was altered by adjusting the Al-waste ratio. This modification occurred in the design of the mixture. Additionally, the value of M of NaOH was set as 11. While the proportion in the mix was enhanced, it was observed that this amount of variation tends to decrease.

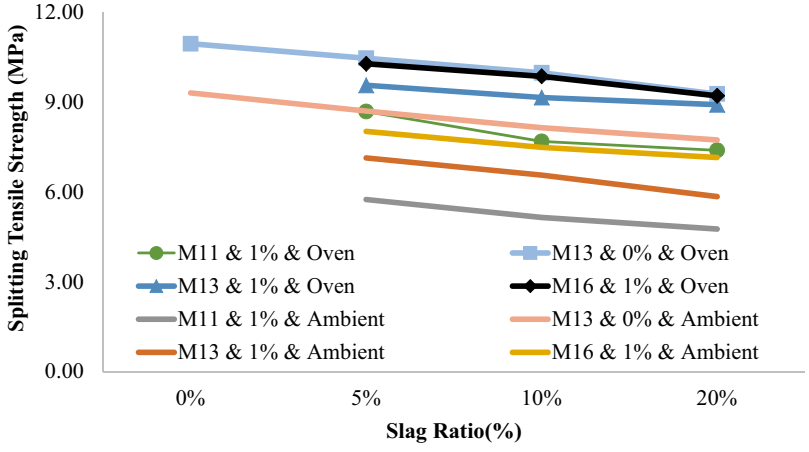

Figure 5: STS test results.

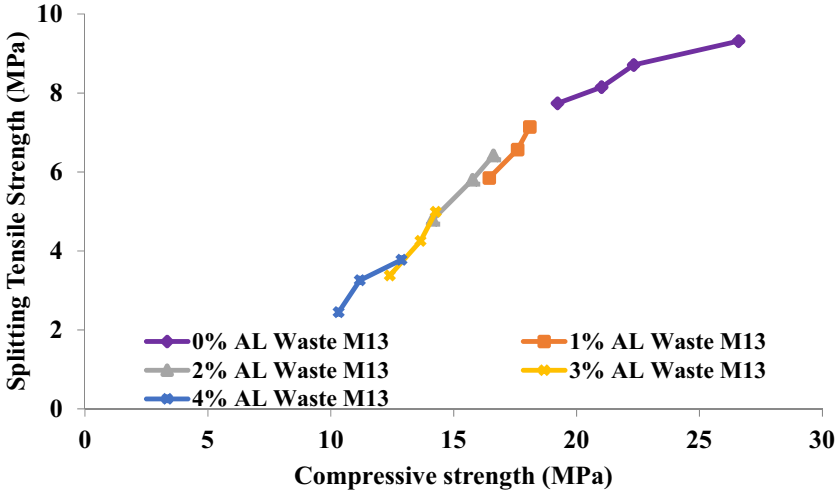

Figure 6: STS *via* CS test results.

In this setup, the proportion of variation in FS was recognized to be 12.74, 17.08, and 21.21%.

Moreover, the percentage of M of NaOH was set as 13, and the percentage of Al-waste with FA was varied from 0 to 4%, with 5% in the GPC mix. In this mixture, the amount of variation in FS was recognized to be 47.25% for 5% slag ratio, 56.29% for 10% slag ratio, and 62.04% for 20% slag ratio. When the amount of Al-waste in this mixture was chosen as 1%, and the amount of slag ratio in the mixture was enhanced from 0 to 20%, it was noticed that the FS of the mix decreased by 25.55%. It was noticed that the FS of the mix decreased significantly.

Moreover, the M of NaOH was consistently chosen as 16. While the percentage of slag in the mix was improved from 0 to 20%, it was noticed that the FS of the mix decreased by 18.53% (from 3.13 to 2.55). It was noticed that the FS of the mix reduced by 14.11% when the amounts of Al-waste in the mix increased from 0 to 1% and the slag ratio was chosen as 20%. In this investigation, the percentage of Al-waste aggregate with FA was kept constant, and the M of NaOH in the mix was altered to 11, 13, and 16 M, as shown in Table 5. The results of this study are presented in Table 5. In addition, as can be seen from Table 5, the percentage of Al-waste aggregate with FA was altered many times to obtain values of 0, 1, 2, 3, and 4%, while the M of NaOH was maintained at 11 M, 13, and 16 M in the concrete mix. FS reduced as the M of the mix rises, as presented in Figure 7. The results show that increasing the heat curing temperature increases the CS and FS of almost all samples. This is similar to the studies conducted in the literature [45]. Extending the heat curing duration and elevating the temperature provide a more conducive environment for the development of GP gels [46]. Because of the non-dissolved particles in the gelatinous matrix of materials, a high alumina concentration will induce fractures and a more heterogeneous microstructure, which will lower the strength [47].

Table 5: FS test results (MPa)

Al-waste (%)	Slag ratio 0%	Slag ratio 5%	Slag ratio 10%	Slag ratio 20%
NaOH (11 M)				
0	2.57	2.51	2.40	2.31
1	—	2.19	1.99	1.82
NaOH (13 M)				
0	2.78	2.65	2.54	2.45
1	—	2.37	2.22	2.15
2	—	1.80	1.59	1.34
3	—	1.46	1.28	1.12
4	—	1.25	1.11	0.93
NaOH (16 M)				
0	3.13	2.94	2.79	2.55
1	—	2.42	2.33	2.19

3.6 Mechanical property correlations of Al-waste

Concrete specimens' CS to STS and CS to FS are shown graphically in Figure 8. Figure 8 shows the results of a linear regression study comparing the compressive-STSs of two samples: 0% Al-waste M11 and 1% Al-waste M11. The correlation values for the two samples are R = 0.9213 and R = 0.9845, respectively. It was determined that the correlation relationship between 0% Al-waste M61 and

1% Al-waste M16 was R = 0.9624 and R = 0.9839. The correlation association between 0% Al-waste M11 and 1% Al-waste M11 was determined to be R = 0.9913 and R = 0.9992, respectively, when looking at the linear regression study between CS and FTS, as shown in Figure 8. The correlation relationship between 0% Al-waste M16 and 1% Al-waste M16 was determined to be R = 0.9912 and R = 0.9802, respectively, when the linear regression analysis between CS and FTS is shown in Figure 8. Within the scope of this investigation, there exist significant correlations that exceed 95% for the predicted links.

3.7 Thermal gravimetric analysis (TGA)

TGA is an analytical method that monitors the change in weight of materials as a result of temperature changes. Thanks to this technique, information about the composition and properties of the material is obtained. Through TGA, thermal behaviors of materials such as degradation, thermal decomposition, water loss, and gas absorption are generally observed. The temperature for the sample to be analyzed is increased within a predetermined program. As the sample heats up, changes such as evaporation, decomposition, and oxidation occurring on the material can cause mass loss or gain. The weighing device continuously records the weight changes of the sample. Thus, the obtained data give information about the thermal behavior of the material when correlated with temperature.

The results presented in Figure 9 illustrate the behavior of the provided sample as it undergoes thermal changes from 0 to 600°C. The blue line depicts the alteration in mass. As the temperature of the initial 9.528 g sample reached 600°C, its mass decreased to approximately 94%, resulting in a 6% loss of mass. In the TGA analyses conducted by Chouksey *et al.* [48] and Aliabdo *et al.* [49] for GPC, mass losses of 6–8% and 9–13% were observed upon heating to 800 and 900°C, respectively. This comparison leads to the inference that the achieved outcomes can be more favorably appraised due to their reduced mass loss [48,49].

It was emphasized that the mass loss detected between 100 and 200°C is primarily attributed to the release of physically and chemically bound water. In the 200–600°C range, the weight reduction is considered to result from the decomposition of residual organics and weakly bonded phases [50,51]. Mass changes occurring above 600°C were interpreted as being indicative of partial structural degradation. The differential thermal analysis (DTA) outcomes are illustrated by the green line in the chart. This leads to a peak within the DTA curves. The peak around 500°C in the DTA thermogram is indicative of a phase transition. Derivative thermogravimetry (DTG) involves calculating the rate of change of a material's temperature with respect to time. Essentially, it quantifies how swiftly the material's temperature changes. Within this technique, the alterations in temperature as a material's temperature is systematically elevated are documented. Fundamentally, its purpose is to determine the material's thermal transitions between phases. As depicted by the red line in the diagram, the DTG outcome demonstrates the points of lowest and highest temperature fluctuations in the sample as time progresses [48].

3.8 Examination with a scanning electron microscope

To evaluate the microstructural properties of the GPC specimens, scanning electron microscopy (SEM) analysis was performed. The SEM images presented in Figure 10a–f

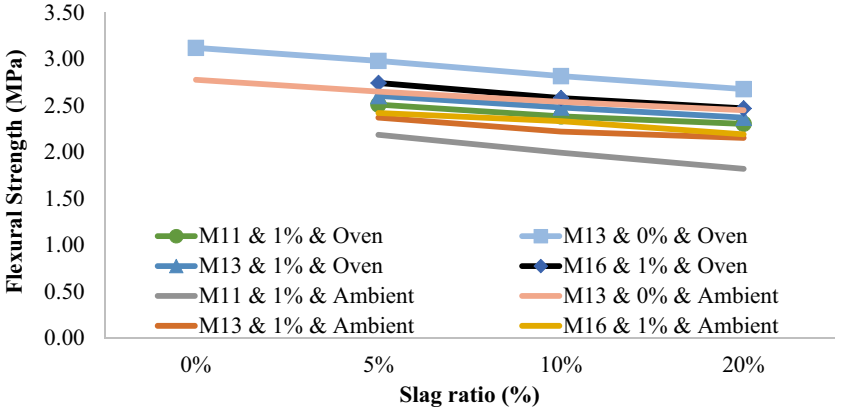

Figure 7: FS test consequences.

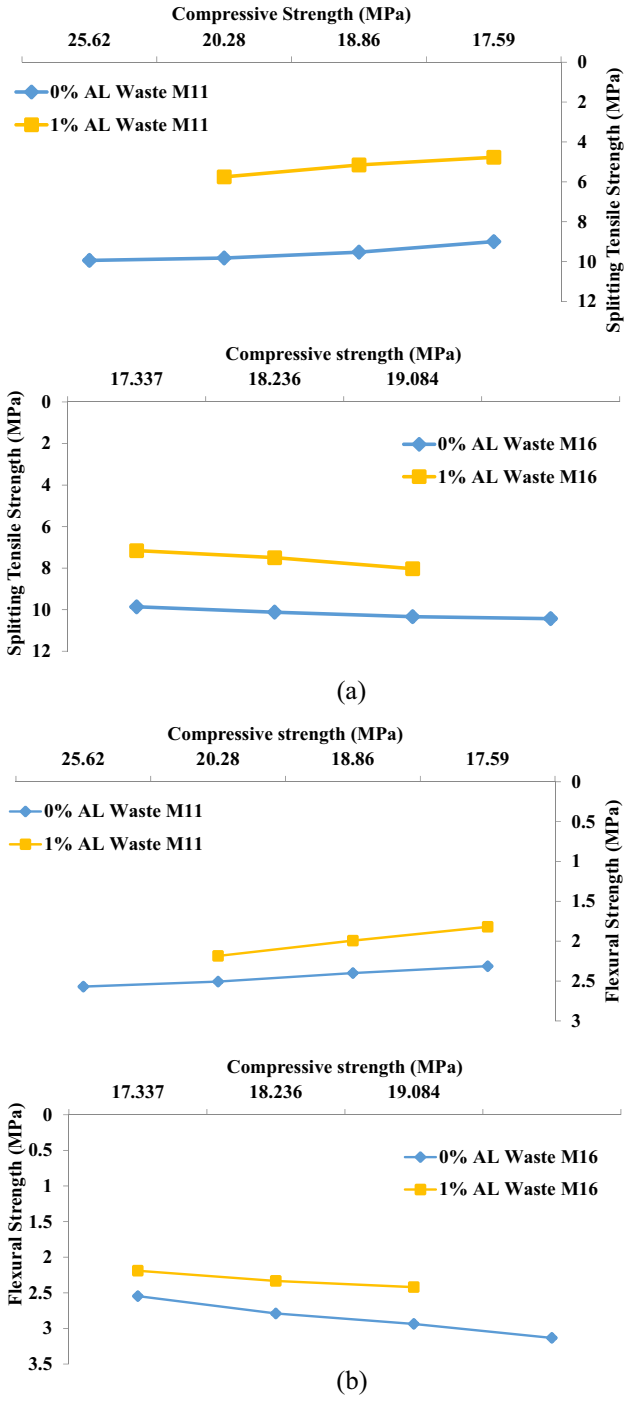

Figure 8: Relation between CS and STS (a) and between CS and FTS (b).

provide a detailed illustration of the effects of Al-waste addition on the internal structure. Figure 10a shows the microstructure of the control specimen without Al-waste. Numerous pores and unreacted FA particles are observed. This indicates incomplete geopolymerization and insufficient formation of binding gel, which may negatively affect the mechanical strength. In Figure 10b, distinct N–A–S–H formation is evident, along with the presence of a GP gel. This structure suggests the development of a hybrid binding system resulting from both geopolymerization and the presence of calcium-containing components. However, the existence of microcracks may be attributed to internal stresses or volumetric changes during setting or curing, potentially compromising long-term durability. Figure 10c and d corresponds to specimens containing Al-waste. A more porous structure is evident in these images. The observed pores are considered to result from the foaming effect caused by the release of hydrogen gas when Al-waste reacts in the alkaline environment. Increased porosity, particularly at higher Al contents, can adversely affect mechanical properties such as strength and density. Figure 10e displays a magnified view of Al fibers. The distribution and orientation of these fibers within the matrix can positively influence mechanical performance by inhibiting crack propagation and improving impact resistance. However, the effectiveness of this contribution depends on the dosage and the fiber–matrix interfacial bonding. Additionally, the formation of C–A–S–H positively affects the strength gained by the concrete after it hardens. Figure 9f focuses on the aggregate–matrix interface. As shown in Figure 10f, the incorporation of Al shavings into the GP matrix affects the interfacial transition zone (ITZ) formed between the aggregate and the binder phase. According to the literature, metals can form either strong or weak ITZ structures with the binder, depending on their surface reactivity and passivation tendencies within the GP environment. In this context, the uneven distribution of Al particles, surface oxidation, and corrosive reactions in an alkaline environment can lead to regions of low bond strength. Consequently, cracks are more likely to initiate and propagate at these weak points under mechanical load [52]. The microstructural integrity of this region is critical for effective load transfer and has a direct impact on the overall mechanical performance [28,53–55]. The high CaO content slag leads to the formation of C–S–H and C–A–S–H gel phases alongside the conventional N–A–S–H gel within the GP matrix. This hybrid gel system enhances early-age strength and contributes to a denser and more durable microstructure. In particular, C–A–S–H gels improve water impermeability and ductility. However, potential long-term issues such as alkali carbonation, thermal instability, and phase separation may arise. Therefore, the quantity and stability of these gel phases in slag-blended GPs should be carefully optimized [56,57].

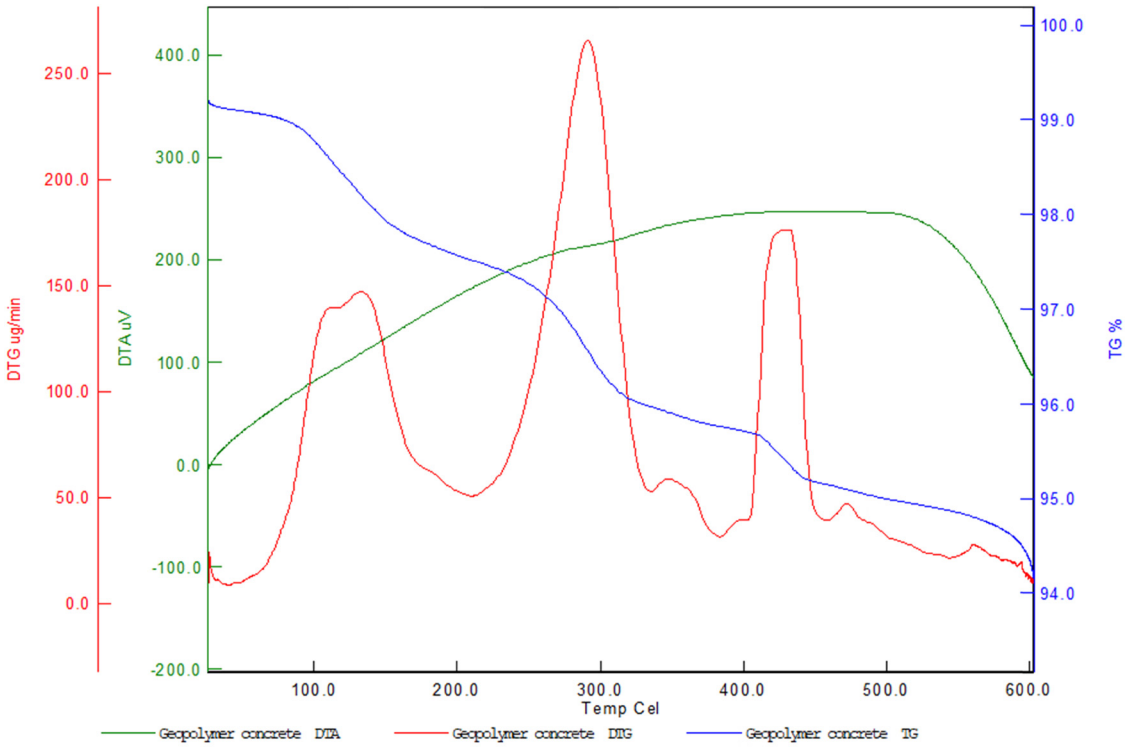

Figure 9: TGA of the GPC sample.

3.9 Evaluation with energy dispersive X-ray (EDX) analysis

EDX analysis, also known as or electron scattering X-ray analysis, is a material characterization technique used to detect the composition present on the surface of a sample. By directing a thin beam of electrons onto or into the sample, various interactions are initiated in the sample. EDX analysis uses these emitted X-rays to understand the chemical composition of the elements present in the sample. Each element exhibits a distinct X-ray energy spectrum. EDX analysis detects these energy spectra to determine the type and abundance of elements in the sample [32,58,59]. In Figure 10, the contents of elements Al, Si, O, Ca, Fe, Na, K, and C resulting from EDX analysis are presented in terms of weight and percentage. The presence of elements in Al-containing GPC has been demonstrated within the scope of this EDX study.

In the sample (Figure 11a), Al(K): 9.56% (weight). In Figure 11b, Al(K): 6.14%. The increase in Al content shows that metallic Al doping in chip form is directly reflected in EDX analysis. This suggests that adding Al strengthens the aluminosilicate structure during geopolymerization reactions by increasing the formation of Al–O–Si bonds, which improves the matrix integrity. Regarding silicon (Si) content, Si(K) in sample A: 19%; Si(K) in sample B: 20.55%. A significant increase in Si content is observed with the addition of Al-waste. This indicates that the interactions between alumina and silica in the matrix are more intense and favor the formation of C–A–S–H or N–A–S–H-like geopolymeric gel phases. The presence of sodium (Na) among the other elements reflects the effect of the activators (NaOH and Na_2SiO_3). A slight decrease in the calcium (Ca) and iron (Fe) ratios was observed with the addition of Al-waste. This suggests that the matrix is concentrated on Al and Si, and the influence of other elements is reduced. From the SEM images, a denser and more compact microstructure is observed in sample B, suggesting tighter interparticle bonding. This finding supports the hypothesis that the addition of Al-waste improves matrix integrity.

The Al CNC waste used in this study had various effects on the GP system with high alkali content at both the chemical and physical levels. The following reaction occurs when metallic Al interacts with strong bases, such as NaOH: this reaction forms sodium aluminate [$NaAl(OH)_4$] solutions and releases a significant amount of hydrogen gas.

$$2Al + 2NaOH + 6H_2O \rightarrow 2Na[Al(OH)_4] + 3H_2. \quad (1)$$

This reaction results in the formation of sodium aluminate ($NaAl(OH)_4$) solutions and the release of a significant amount of hydrogen gas. This accelerates the

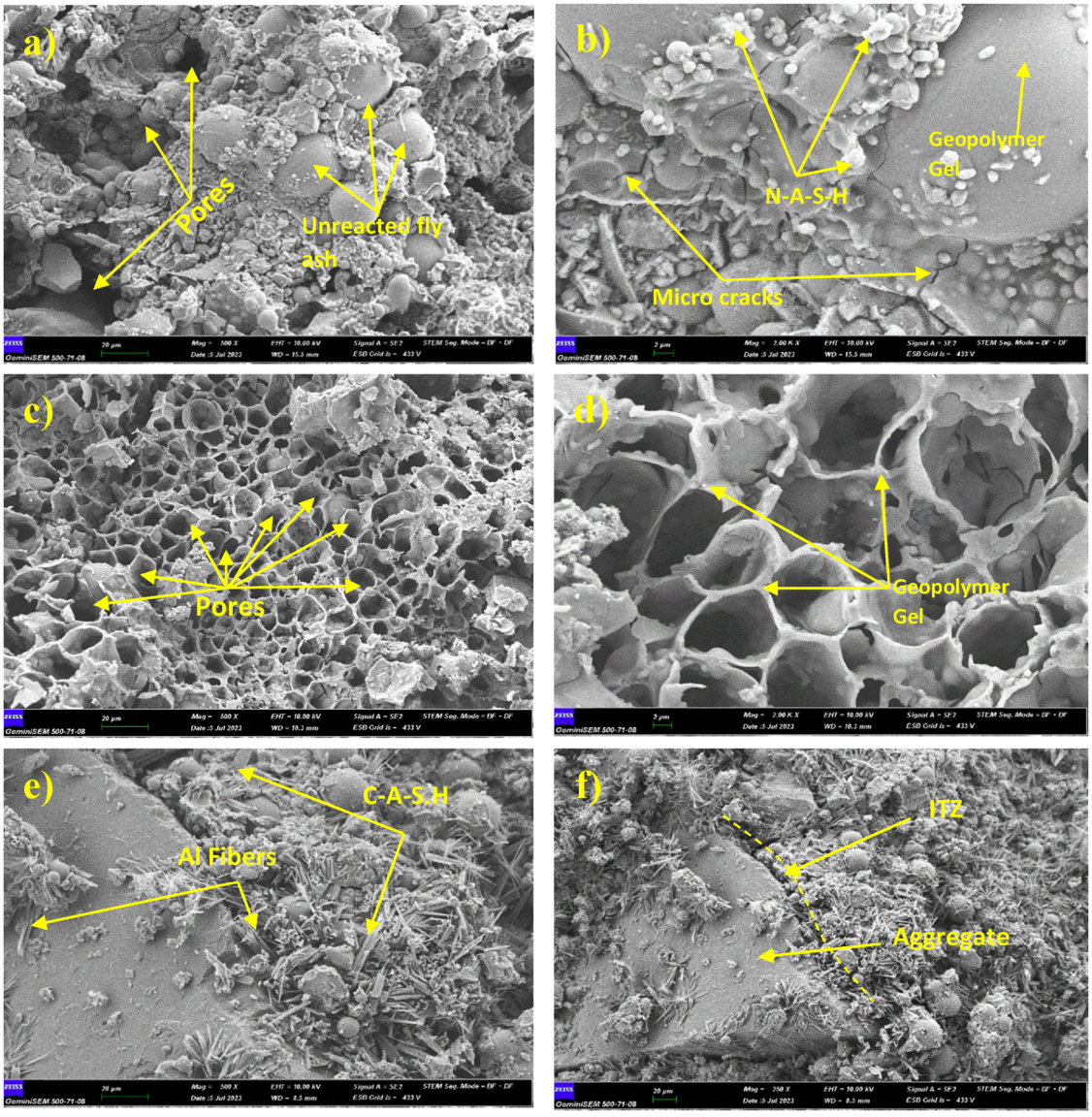

Figure 10: SEM micrographs of the obtained samples.

geopolymerization mechanism by increasing the ambient pH, contributing to the formation of Si–O–Al bonds at an earlier stage and shortening the setting process. Additionally, Al particles are quickly surrounded by GP gel phases, creating a passivation effect on their surfaces. This passivation prevents both further reaction of the particles and excessive porosity in the system. At the same time, these surface layers act as nucleation centers that promote the growth of gel phases and homogeneous matrix formation. This can positively affect strength increase, especially at early stages. Particle size distribution also plays a decisive role in these interactions. The exothermic reactions observed due to Al doping caused local temperature increases and accelerated gel phase formation, reducing the setting time. However, uncontrolled hydrogen gas outgassing can lead to pore formation, resulting in a decrease in mechanical strength. Therefore, control mechanisms related to particle size, distribution, and surface reactions are critical for system performance. Further studies on this subject can be conducted. In conclusion, SEM images and EDX analyses demonstrate that Al doping is homogeneous within the GP matrix. In conclusion, SEM and EDX analysis demonstrate that Al doping can be homogeneously dispersed in the GP matrix and integrated with silicate-based phases. Under appropriate conditions, the Al sawdust additive can accelerate geopolymerization processes, shorten the setting time, and increase the final mechanical strength.

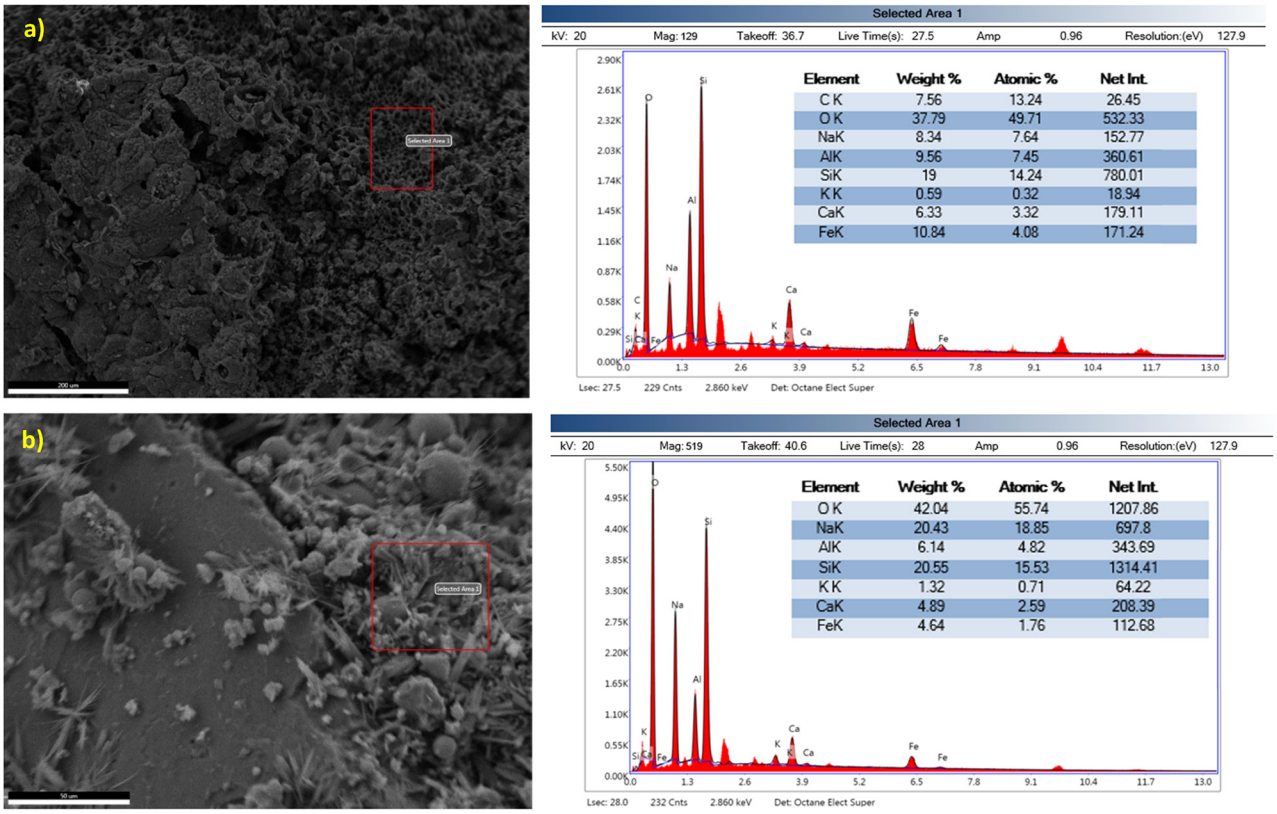

Figure 11: EDX spectra of the obtained samples. (a) EDX-1 and (b) EDX-2.

4 Concluding remarks

In this evaluation research, FA was partially replaced with GBFS in the production of GPC. Additionally, Al-waste was separately incorporated into the mixtures at rates ranging from 0 to 4%. The M of the NaOH solution was selected as 11, 13, and 16 M, and the effects of these variables on mechanical and microstructural properties were investigated. CS, STS, and FS were evaluated on the hardened specimens, and SEM analysis was conducted to examine and compare the microstructural characteristics of the samples.

- It was determined that increasing the M of NaOH negatively affected the workability of the mix. Additionally, the addition of Al-waste caused a significant decrease in slump values. The setting time was recorded as approximately 10 min when Al-waste was added at 1, 2, and 3%, while it increased to around 40 min with 4% addition. As a result of these implications, the slump values decreased as the M increased. In addition, the impact of the Al-waste ratio on the slump was studied while maintaining the same M throughout the experiment. It was revealed that the slump values dropped whenever there was an increase in the percentage of Al-waste.
- The M of NaOH was selected as 11, 13, and 16 M, while the proportion of Al-waste and slag ratio in the GPC mixture were varied at 0, 1, 2, 3, 4% and 0, 5, 10, and 20%. Experimental results indicated that increasing the M of NaOH proportionally amplified the variations in mechanical properties. Moreover, increasing the slag content from 0 to 20% led to a reduction in CS by 31.34% at 11 M and 1% AL waste and by 27.68 and 30.94% at 13 and 16 M and 1% AL waste, respectively.
- When the Al-waste content was increased from 0 to 1%, a 17.66% reduction in CS was observed for 11 M. At molarities of 13 and 16 M and 5% slag ratio, elevating the Al-waste content to 4% resulted in CS reductions of approximately 42.31 and 33.79%, respectively.
- Analysis of the results revealed that STS generally exhibited a trend parallel to that of CS. Despite increases in the mixture proportion from 0 to 20% slag ratio, the percentage change in STS decreased to 9.45% at 11 M and 0% AL waste. Furthermore, increasing the slag content from 0 to 20% resulted in STS decreases of 16.86 and 5.46% at molarities of 13 and 16 M, respectively.
- NaOH M was maintained at 11, 13, and 16 M, with Al-waste content ranging from 0 to 4%. It was observed

that STS decreased as the Al-waste proportion increased from 0 to 4%.
- Microstructural analyses and SEM imaging revealed that the incorporation of Al into GPC induced pore formation due to swelling. EDX analysis confirmed the presence of elements such as Al, Si, O, Ca, Fe, Na, K, and C. TGA results demonstrated approximately 94% mass retention upon heating to 600°C, indicating lower mass loss compared to values reported in the literature.
- Throughout the experimental procedure, while the Al-waste ratio was kept constant, the M of NaOH was adjusted to 11 M, 13 M, and 16 M. It was noted that increases in M correlated with reductions in observed fluctuations, a trend that was also valid under inverse conditions.

Acknowledgments: The authors are thankful for the financial support provided for this research by the Deanship of Scientific Research at King Khalid University, Abha, Saudi Arabia, through Large Groups RGP2/539/46.

Funding information: This research was supported by the Deanship of Scientific Research at King Khalid University, Abha, Saudi Arabia, through Large Groups RGP2/539/46.

Author contributions: Ali İhsan Çelik: investigation, formal analysis, visualization, writing – original draft, conceptualization. Ufuk Tunç: investigation, formal analysis, writing – original draft, data curation. Memduh Karalar: investigation, formal analysis, writing – original draft, writing – review and editing. Essam Althaqafi: writing – original draft, funding acquisition, visualization, data curation. Yasin Onuralp Özkılıç: writing – original draft, writing – review and editing, investigation, formal analysis, conceptualization, methodology. All authors have accepted responsibility for the entire content of this manuscript and approved its submission.

Conflict of interest: The authors state no conflict of interest.

Data availability statement: All data generated or analyzed during this study are included in this published article.

References

[1] Scrivener, K. L., V. M. John, and E. M. Gartner. Eco-efficient cements: Potential economically viable solutions for a low-CO_2 cement-based materials industry. *Cement and Concrete Research*, Vol. 114, 2018, pp. 2–26.

[2] Snellings, R., P. Suraneni, and J. Skibsted. Future and emerging supplementary cementitious materials. *Cement and Concrete Research*, Vol. 171, 2023, id. 107199.

[3] Sukontasukkul, P., D. Intarabut, T. Phoo-ngernkham, C. Suksiripattanapong, H. Zhang, and P. Chindaprasirt. Self-compacting steel fibers reinforced geopolymer: Study on mechanical properties and durability against acid and chloride attacks. *Case Studies in Construction Materials*, Vol. 19, 2023, id. e02298.

[4] Davidovits, J. Geopolymer chemistry and applications. Inst Geopolymere, Saint-Quentin, Fr, 2008.

[5] Parathi, S., P. Nagarajan, and S. A. Pallikkara. Ecofriendly geopolymer concrete: A comprehensive review. *Clean Technologies and Environmental Policy*, Vol. 23, 2021, pp. 1701–1713.

[6] Duxson, P. and J. L. Provis. Designing precursors for geopolymer cements. *Journal of the American Ceramic Society*, Vol. 91, No. 12, 2008, pp. 3864–3869.

[7] Feng, Z., P. Zhang, J. Guo, Y. Zheng, and S. Hu. Single and synergistic effects of nano-SiO_2 and hybrid fiber on rheological property and compressive strength of geopolymer concrete. *Construction and Building Materials*, Vol. 472, 2025, id. 140945.

[8] Shilar, F. A., M. A. Shilar, and S. V. Ganachari. Advancing sustainable construction: Bamboo fibers in clay-based geopolymer composites. *Journal of Building Engineering*, Vol. 104, 2025, id. 112247.

[9] Zhang, P., Z. Wen, X. Han, J. Guo, and S. Hu. A state-of-the-art review on frost resistance of fiber-reinforced geopolymer composites. *Sustainable Chemistry and Pharmacy*, Vol. 45, 2025, id. 102006.

[10] Shilar, F. A., S. V. Ganachari, V. B. Patil, N. Almakayeel, and T. M. Y. Khan. Development and optimization of an eco-friendly geopolymer brick production process for sustainable masonry construction. *Case Studies in Construction Materials*, Vol. 18, 2023, id. e02133.

[11] Amin, M., Y. Elsakhawy, K. Abu el-hassan, and B. A. Abdelsalam. Behavior evaluation of sustainable high strength geopolymer concrete based on fly ash, metakaolin, and slag. *Case Studies in Construction Materials*, Vol. 16, 2022, id. e00976.

[12] Li, W., E. D. Shumuye, T. Shiying, Z. Wang, and K. Zerfu. Eco-friendly fibre reinforced geopolymer concrete: A critical review on the microstructure and long-term durability properties. *Case Studies in Construction Materials*, Vol. 16, 2022, id. e00894.

[13] Gülmez, N. Reuse of industrial metal wastes as partial replacement of aggregates in mortar production. *Dicle Üniversitesi Mühendislik Fakültesi Mühendislik Dergisi*, Vol. 12, No. 5, 2021, pp. 875–880.

[14] Ozkilic, Y. O., O. Zeybek, A. I. Celik, E. Althaqafi, M. A. O. Mydin, A. Dulaimi, et al. Fresh and hardened properties of expansive concrete utilizing waste aluminum lathe. *Steel and Composite Structures*, Vol. 50, No. 5, 2024, pp. 595–608.

[15] Almeshal, I., Y. O. Özkılıç, C. Aksoylu, M. Karalar, and M. Alharthai. Ductility and strength of reinforced concrete beams strengthened with aluminum CNC waste. *Structural Concrete*, Vol. 25, No. 5, 2024, pp. 3232–3245.

[16] Özkılıç, Y. O., M. Karalar, C. Aksoylu, A. N. Beskopylny, S. A. Stel'makh, E. M. Shcherban, et al. Shear performance of reinforced expansive concrete beams utilizing aluminium waste. *Journal of Materials Research and Technology*, Vol. 24, 2023, pp. 5433–5448.

[17] Mohammadyan-Yasouj, S. E., N. Heidari, and H. Shokravi. Influence of waste alumina powder on self-compacting concrete resistance under elevated temperature. *Journal of Building Engineering*, Vol. 41, 2021, id. 102360.

[18] Rahim, N. L., N. M. Ibrahim, S. Salehuddin, R. Che Amat, S. A. Mohammed, and C. R. Hibadullah. The utilization of aluminum waste as sand replacement in concrete. *Key Engineering Materials*, Vol. 594, 2014, pp. 455–459.
[19] Bumanis, G., D. Bajare, A. Korjakins, and D. Vaičiukynienė. Sulfate and freeze-thaw resistance of porous geopolymer based on waste clay and aluminum salt slag. *Minerals*, Vol. 12, No. 9, 2022, id. 1140.
[20] Onutai, S., S. Jiemsirilers, and T. Kobayashi. Geopolymer sourced with fly ash and industrial aluminum waste for sustainable materials. *Waste management: Concepts, methodologies, tools, and applications*, IGI Global Scientific Publishing, Hershey, Pennsylvania, USA, 2020, pp. 676–696.
[21] Xu, H. and J. S. J. Van Deventer. Geopolymerisation of multiple minerals. *Minerals Engineering*, Vol. 15, 2022, pp. 1131–1139.
[22] Abdila, S. R., M. M. A. B. Abdullah, R. Ahmad, S. Z. A. Rahim, M. Rychta, I. Wnuk, et al. Evaluation on the mechanical properties of ground granulated blast slag (GGBS) and fly ash stabilized soil *via* geopolymer process. *Materials*, Vol. 14, No. 11, 2021, id. 2833.
[23] Kouamo, H. T., A. Elimbi, J. Mbey, C. N. Sabouang, and D. Njopwouo. The effect of adding alumina-oxide to metakaolin and volcanic ash on geopolymer products: A comparative study. *Construction and Building Materials*, Vol. 35, 2012, pp. 960–969.
[24] Oderji, S. Y., B. Chen, M. R. Ahmad, and S. F. A. Shah. Fresh and hardened properties of one-part fly ash-based geopolymer binders cured at room temperature: Effect of slag and alkali activators. *Journal of Cleaner Production*, Vol. 225, 2019, pp. 1–10.
[25] Pimraksa, K., P. Chindaprasirt, A. Rungchet, K. Sagoe-Crentsil, and T. Sato. Lightweight geopolymer made of highly porous siliceous materials with various Na_2O/Al_2O_3 and SiO_2/Al_2O_3 ratios. *Materials Science and Engineering: A*, Vol. 528, No. 21, 2011, pp. 6616–6623.
[26] Shilar, F. A., S. V. Ganachari, V. B. Patil, T. Y. Khan, and S. D. A. Khadar. Molarity activity effect on mechanical and microstructure properties of geopolymer concrete: A review. *Case Studies in Construction Materials*, Vol. 16, 2022, id. e01014.
[27] Verma, N. K., M. C. Rao, and S. Kumar. Effect of molarity of NaOH and alkalinity ratio on compressive strength of geo-polymer concrete. *Materials Today: Proceedings*, Vol. 64, 2022, pp. 940–947.
[28] Özkılıç, Y. O., A. İ. Çelik, U. Tunç, M. Karalar, A. Deifalla, T. Alomayri, et al. The use of crushed recycled glass for alkali activated fly ash based geopolymer concrete and prediction of its capacity. *Journal of Materials Research and Technology*, Vol. 24, 2023, pp. 8267–8281.
[29] Çelik, A. İ., U. Tunç, A. Bahrami, M. Karalar, M. A. O. Mydin, T. Alomayri, et al. Use of waste glass powder toward more sustainable geopolymer concrete. *Journal of Materials Research and Technology*, Vol. 24, 2023, pp. 8533–8546.
[30] Çelik, A. İ., Y. O. Özkılıç, A. Bahrami, and I. Y. Hakeem. Mechanical performance of geopolymer concrete with micro silica fume and waste steel lathe scraps. *Case Studies in Construction Materials*, Vol. 19, 2023, id. e02548.
[31] López, F. J., S. Sugita, M. Tagaya, and T. Kobayashi. Metakaolin-based geopolymers for targeted adsorbents to heavy metal ion separation. *Journal of Materials Science and Chemical Engineering*, Vol. 2, No. 7, 2014, id. 16.
[32] Çelik, A. İ. Mechanical performance of geopolymer concrete based on basalt and marble powder. *Iranian Journal of Science and Technology, Transactions of Civil Engineering*, Vol. 47, No. 4, 2023, pp. 2173–2187.
[33] Nath, P. and P. K. Sarker. Effect of GGBFS on setting, workability and early strength properties of fly ash geopolymer concrete cured in ambient condition. *Construction and Building Materials*, Vol. 66, 2014, pp. 163–171.
[34] Hardjito, D., S. E. Wallah, D. M. J. Sumajouw, and B. V. Rangan. On the development of fly ash-based geopolymer concrete. *Materials Journal*, Vol. 101, No. 6, 2004, pp. 467–472.
[35] Çelik, A. İ. and Y. O. Özkılıç. Geopolymer concrete with high strength, workability and setting time using recycled steel wires and basalt powder. *Steel and Composite Structures, An International Journal*, Vol. 46, No. 5, 2023, pp. 689–707.
[36] Kumaravel, S. Development of various curing effect of nominal strength Geopolymer concrete. *Journal of Engineering Science and Technology Review*, Vol. 7, No. 1, 2014, pp. 116–119.
[37] Nurruddin, M. F., H. Sani, B. S. Mohammed, and I. Shaaban. Methods of curing geopolymer concrete: A review. *International Journal of Advanced and Applied Sciences*, Vol. 5, No. 1, 2018, pp. 31–36.
[38] Yip, C. and J. Van Deventer. Microanalysis of calcium silicate hydrate gel formed within a geopolymeric binder. *Journal of Materials Science*, Vol. 38, 2003, pp. 3851–3860.
[39] Fang, G., W. K. Ho, W. Tu, and M. Zhang. Workability and mechanical properties of alkali-activated fly ash-slag concrete cured at ambient temperature. *Construction and Building Materials*, Vol. 172, 2018, pp. 476–487.
[40] Görhan, G. and G. Kürklü. The influence of the NaOH solution on the properties of the fly ash-based geopolymer mortar cured at different temperatures. *Composites Part B: Engineering*, Vol. 58, 2014, pp. 371–377.
[41] Hanjitsuwan, S., S. Hunpratub, P. Thongbai, S. Maensiri, V. Sata, and P. Chindaprasirt. Effects of NaOH concentrations on physical and electrical properties of high calcium fly ash geopolymer paste. *Cement and Concrete Composites*, Vol. 45, 2014, pp. 9–14.
[42] Nazari, A., A. Bagheri, and S. Riahi. Properties of geopolymer with seeded fly ash and rice husk bark ash. *Materials Science and Engineering: A*, Vol. 528, No. 24, 2011, pp. 7395–7401.
[43] Somna, K., C. Jaturapitakkul, P. Kajitvichyanukul, and P. Chindaprasirt. NaOH-activated ground fly ash geopolymer cured at ambient temperature. *Fuel*, Vol. 90, No. 6, 2011, pp. 2118–2124.
[44] Manikandan, P. and V. Vasugi. A critical review of waste glass powder as an aluminosilicate source material for sustainable geopolymer concrete production. *Silicon*, Vol. 13, No. 10, 2021, pp. 3649–3663.
[45] Durak, U. The improvement of strength and microstructural properties of fly ash-based geopolymer by adding elemental aluminum powder. *Journal of Material Cycles and Waste Management*, Vol. 25, No. 1, 2023, pp. 157–170.
[46] Atiş, C., E. Görür, O. Karahan, C. Bilim, S. İlkentapar, and E. Luga. Very high strength (120 MPa) class F fly ash geopolymer mortar activated at different NaOH amount, heat curing temperature and heat curing duration. *Construction and Building Materials*, Vol. 96, 2015, pp. 673–678.
[47] Ahmed, M. M., K. El-Naggar, D. Tarek, A. Ragab, H. Sameh, A. M. Zeyad, et al. Fabrication of thermal insulation geopolymer bricks using ferrosilicon slag and alumina waste. *Case Studies in Construction Materials*, Vol. 15, 2021, id. e00737.
[48] Chouksey, A., M. Verma, N. Dev, I. Rahman, and K. Upreti. An investigation on the effect of curing conditions on the mechanical and microstructural properties of the geopolymer concrete. *Materials Research Express*, Vol. 9, No. 5, 2022, id. 055003.
[49] Aliabdo, A. A., M. Abd Elmoaty, and H. A. Salem. Effect of cement addition, solution resting time and curing characteristics on fly ash

based geopolymer concrete performance. *Construction and Building Materials*, Vol. 123, 2016, pp. 581–593.
[50] Instruments, T. A. *High resolution thermogravemetric analysis: a new technique for obtaining superior analytical results*, TA Instruments, New Castle, DE, USA, 1992.
[51] Lothenbach, B., P. Durdzinski, and K. De Weerdt. Thermogravimetric analysis. *A practical guide to microstructural analysis of cementitious materials*, CRC Press, Boca Raton, Florida, USA, Vol. 1, 2016, pp. 177–211.
[52] Alanazi, H. Study of the interfacial transition zone characteristics of geopolymer and conventional concretes. *Gels*, Vol. 8, No. 2, 2022, id. 105.
[53] Khmiri, A., M. Chaabouni, and B. Samet. Chemical behaviour of ground waste glass when used as partial cement replacement in mortars. *Construction and Building Materials*, Vol. 44, 2013, pp. 74–80.
[54] Kim, J., C. Yi, and G. Zi. Waste glass sludge as a partial cement replacement in mortar. *Construction and Building Materials*, Vol. 75, 2015, pp. 242–246.
[55] Luo, Y., Q. Zhang, D. Wang, L. Yang, X. Gao, Y. Liu, et al. Mechanical and microstructural properties of MK-FA-GGBFS-based self-compacting geopolymer concrete composites. *Journal of Building Engineering*, Vol. 77, 2023, id. 107452.
[56] Fernández-Jiménez, A., A. Palomo, and M. Criado. Microstructure development of alkali-activated fly ash cement: A descriptive model. *Cement and Concrete Research*, Vol. 35, No. 6, 2005, pp. 1204–1209.
[57] Provis, J. L. and J. S. J. Van Deventer. *Geopolymers: Structures, processing, properties and industrial applications*, Elsevier, Cambridge, UK, 2009.
[58] Nath, S., S. Maitra, S. Mukherjee, and S. Kumar. Microstructural and morphological evolution of fly ash based geopolymers. *Construction and Building Materials*, Vol. 111, 2016, pp. 758–765.
[59] Albidah, A., M. Alghannam, H. Abbas, T. Almusallam, and Y. Al-Salloum. Characteristics of metakaolin-based geopolymer concrete for different mix design parameters. *Journal of Materials Research and Technology*, Vol. 10, 2021, pp. 84–98.